EXPERIMENTAL INVESTIGATION OF THE ANTI-ICING PROPERTIES OF HYDROPHOBIC SURFACES

Lígia Venancio Froening, ligia.froening@gmail.com
Higuel Parga de Paiva Norões, higuel.noroes@gmail.com
Pedro Silva Petindá, pedro.petinda@poli.ufrj.br
Juliana Braga Rodrigues Loureiro, jbrloureiro@mecanica.coppe.ufrj.br
Interdisciplinary Center for Fluid Dynamics (NIDF), Federal University of Rio de Janeiro, C.P. 68503, 21.945-970 - Rio de Janeiro – Brazil

Abstract. *Icing is a phenomenon that may occur in power lines, wind turbines and aircrafts causing detrimental effects which may result in catastrophic failures. Typical anti-icing techniques are based on heating systems, which increases the operating cost or reduce the operating efficiency of the engineering application. Since the early sixties, the use of hydrophobic and superhydrophobic surfaces is being investigated as an alternative anti-icing solution. The objective of this work is to quantify the behavior of a hydrophobic surface subjected to different water droplets size distributions, under a range of Reynolds numbers and flow temperatures. For this purpose, a control surface made by aluminun sheet and the hydrophobic coated surface were characterized in the Climatic wind-tunnel of NIDF/COPPE/UFRJ, which is capable of simulating extreme atmospheric conditions such as low temperatures, high velocities and different humidity conditions. Droplet diameter distribution was characterized with the aid of a Shadow Sizer System. Furthermore, high-speed camera images were used to quantify the ice accretion evolution on the hydrophobic surface.*

Keywords*: Wind-tunnel, icing, hydrophobic surface, droplet size distribution.*

1. INTRODUCTION

Icing is a phenomenon that may occur in power lines, wind turbines and aircrafts, causing detrimental effects which may result in catastrophic failures. Ice accretion on a turbine, for instance, may reduce its efficiency due to changes in its original designed profile. Ice accumulation on wings and empennage can happen either during the flight or on the ground, when solutions are need for ice prevention and removal. Hence, due to the risks offered to security and flight performance downgrade, this phenomenon poses a critical issue for the aeronautic sector.

Typical anti-icing techniques are based on heating systems, which increases the operating cost of flight and reduce the operating efficiency of aircraft turbines. Since the early sixties, the use of hydrophobic and superhydrophobic surfaces is being investigated as an alternative anti-icing solution. The development of new ice/water-repellent surfaces, or the combination of coating application and low power heating systems can render more efficient solutions for the industrial sector. In particular, the application of hydrophobic coatings may reduce flight costs not only by reducing the power required for the de-icing heating system but also by decreasing the surface drag. In fact, recent investigations are focusing on the fabrication of drag reducing surfaces that have intrinsic water-repellent characteristics.

Literature provides a number of works dedicated to study the influence of surface coatings on the reduction of ice adhesion strength and on the delay in ice accretion time (Yeong *et al.*, 2015; Alizadeh *et al.*, 2012; *Yung et al.*, 2011). However, the majority of the available investigations are restricted to small scale experiments of droplets impinging on a cooled surface. Studies conducted for dynamics conditions with cloud simulated droplets are rarely found in literature (Antonini *et al.*, 2011; Fortin *et al.*, 2011).

The purpose of this work is to investigate the effects that hydrophobic surfaces exert on the ice accretion phenomenon, considering the influence of the turbulent flow that drives the droplet impact. Experiments have been performed on the Climatic Wind Tunnel (NIDF/UFRJ) with the aid of a spray bar system that can simulate atmospheric supercooled large droplets. A commercial hydrophobic paint was used to coat an aluminum airfoil that was compared to the reference unpainted surface. Measurements of flow velocity, droplet size distribution, contact angle and ice accreted shape are presented.

Fortin *et al.* (2011) evaluated the behavior of hydrophobic and superhydrophobic surfaces during icing Wind tunnel tests. In their experiments, authors combined the coatings with an internally heated airfoil in order to quantify the resulting energy savings. The reported cost reduction was 33% for glaze ice and 13% for rime ice in comparison anti-ice system with no coating. The work concludes that the water-repellent coatings favor water running without freezing over unheated areas. As so, the higher the contact angle, the better performance the surface would have.

A similar work has been developed by Antonini *et al.* (2011), who have also studied a heated airfoil in an icing wind tunnel. Authors observed a reduction of up to 80% of the energy required to prevent ice accretion on the wing. The shedding of drops is also pointed out as key controlling mechanism to prevent ice formation.

However, this result is not widely accepted, since recent studies have shown that an increase in contact angle does not always improve anti-icing coating performance (Yeong *et al.*, 2015; Bharathidasan *et al.*, 2014; Teisala *et al.*, 2012).

Yeong *et al.* (2015) used a cold chamber with a single spray nozzle to measure the ice adhesion strength on hydrophobic and superhydrophobic surfaces. This work reports that the ice adhesion on superhydrophobic surfaces was not influenced by wettability parameters, such as contact angle, but depended primarily on a surface topology parameter, that quantifies the wavelength of surface features, or roughness.

Oberli *et al.* (2014), on the other hand, investigated ice accretion from the point of view of crystal nucleation and growth over a surface. The authors observed that imperfections or vacancies on the surface can accumulate water condensate in the form of micro-droplets. It has been observed that ice crystals seed ice formation in the neighboring water droplets upon contact. Their conclusion is that "the nucleation mechanism of ice in the condensed water micro-droplets influence the freezing delay and should be the subject of future experimental investigations to elucidate the problem".

2. EXPERIMENTAL SETUP

2.1 Climatic Wind Tunnel

The experiments were performed at the Climatic Wind Tunnel of the Interdisciplinary Center for Fluid Dynamics (COPPE/UFRJ), which was designed to simulate critical atmospheric cloud conditions. This is a closed loop wind tunnel that is 9 m long, 4 m high and is made of insulated stainless steel. Mach numbers up to 0.3 and temperatures as low as −15 ^{o}C can be achieved. Its test section is 2 m long and has a cross section of 300 mm x 300 mm. The vertical walls of the test section are made by a double-glazed glass window equipped with a heating system in order to prevent condensation and to allow the use of optical measurement techniques.

An overview of the Climatic Wind Tunnel is shown in Figure *1*. The evaporator is located on the upper side of the closed loop. After passing the evaporator the airflows through guiding vanes on each corner and then reaches the honeycomb, the screens and the contraction section, where the spray bar system is located.

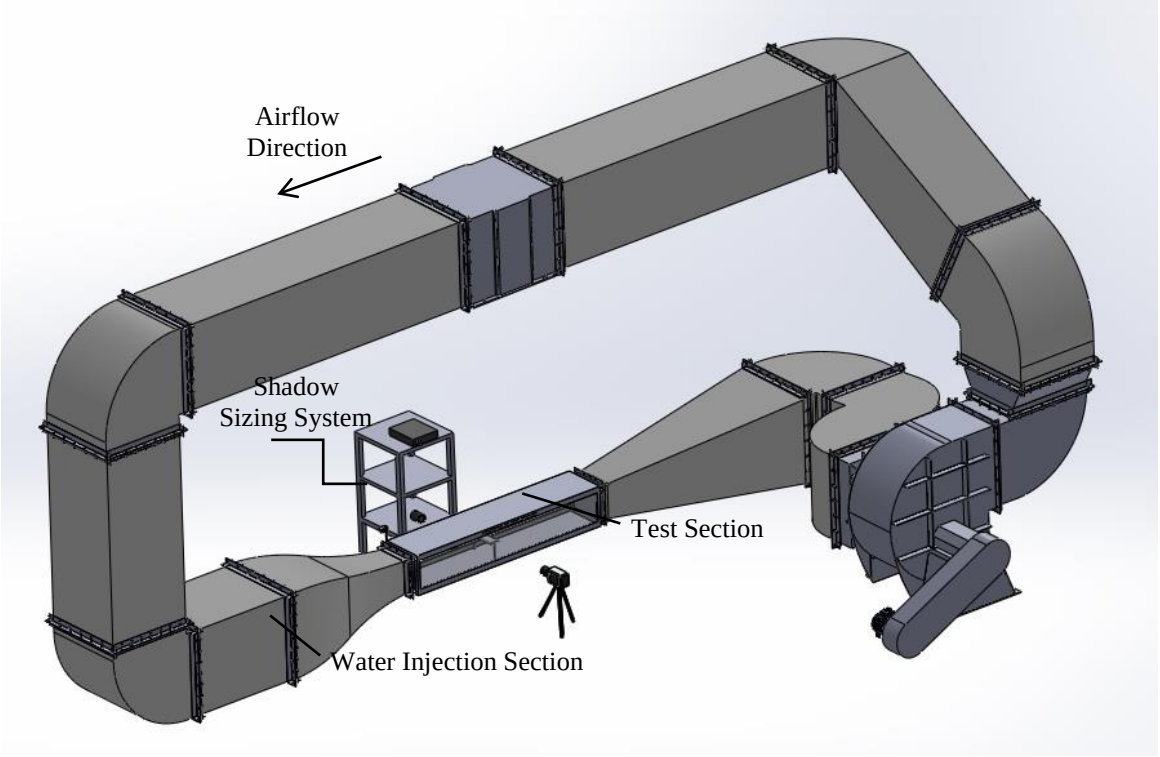

Figure 1: Overview of the Climatic Wind Tunnel (NIDF/UFRJ).

The spray bar system is comprised of five independently controlled nozzles, which were distributed in three horizontal bars along the cross section of the contraction. The position of each nozzle was adjusted in order to generate a uniform cloud distribution at the test section. The droplet size distribution can be controlled by the air and water flow rates and pressures on the nozzle inlet.

2.2 Instrumentation

A Shadow Sizer System, from Dantec Dynamics, was used to quantify the droplet size distribution along the incoming flow and to characterize the shape of the ice accreted of the tested surfaces. This system is composed by the high speed camera Nanosense MKIII, with resolution of 1024x1024 pixels and maximum frame rate of 5 kHz. The light source is provided by a Constellation led light, made by a matrix of 32 x 32 individual white LEDs. A diffusive paper was positioned in front of the led array in order to provide a diffusive background illumination to the droplet particles. The software Dynamic Studio version 3.20 was used for image treatment and diameter calculation. Typically, image background subtraction was applied to increase contrast. Afterward, a median filter is applied followed by a binarization step. The Shadow Sizer processing is based on contour detection algorithm and then furnishes equivalent diameter, area and perimeter, as well as velocity vector for each measured droplet. In order to quantify particles of the size of few hundreds of microns, a 200 mm f/2.8D micro Nikkor lens was used. This allowed high magnification in a small distance from the test section. A sketch of the Shadow System installed at the test section is illustrated in Figure 2. Contact angles have also been measured with the aid of the Shadow Sizer System, as will be described in the results.

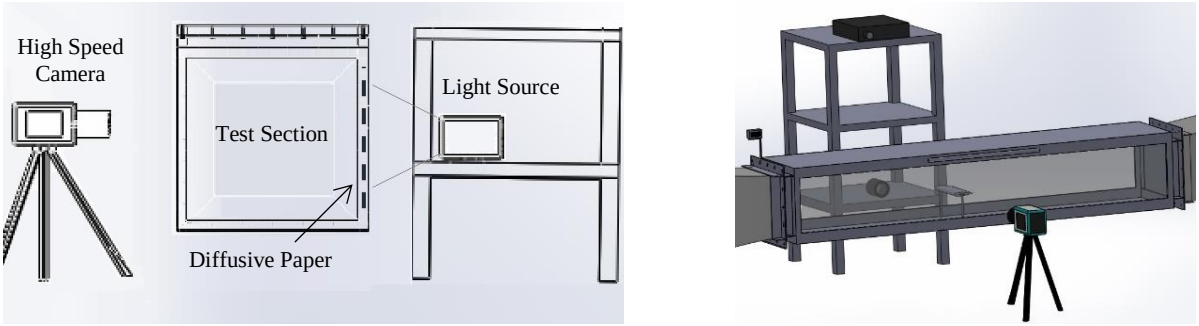

Figure 2: Illustration of the Shadow Sizer System installed at the test section, where the wing model is installed.

A 2D PIV System from Dantec Dynamics is also available for mean velocity and turbulence statistics measurement. After a detailed literature review, no investigation was found about the influence of the turbulent flow field on the properties of water-repellent surfaces. As will be discussed in the next section, the droplet impingement on the hydrophobic surface is followed by a bouncing effect, which favors droplet entrainment by the incoming airflow. When in contact with the coated surfaces, water droplets are easily removed by the flow, diminishing water content that remains attached to the surface and, as a consequence, decreasing ice accretion. This phenomenon has been reported by Antonini *et al.* (2011) and by Fortin *et al.* (2011). However, none of these works have reported data on turbulence statistics of the mean flow field. In fact, entrainment and skin friction are scaling parameters directly related to the turbulent flow field.

2.3 Experimental conditions

The reference and the hydrophobic airfoils investigated in the Climatic Wind Tunnel are made from a polypropylene frame that followed a NACA 0021 profile. The models have constant section of 235 mm long and 200 mm chord length. The polypropylene frame has five ribs and two spars that were manufactured by a 3D Stratasys printer and then covered by a thin sheet of aluminum, which was deformed and glued to the frame.

The reference model was kept with the industrial smooth surface from the original aluminum sheet. The hydrophobic model was coated by spraying a commercial paint (*Ultra-ever Dry*, from UltraTech International, Inc.) on the aluminum sheet prior to its attachment to the NACA frame.

Although the painting procedure is done very carefully, some imperfections may appear due to a lack of uniformity in the spray system. These imperfections are not clearly visible but can be easily identified since water droplets adhere to these defect points. As pointed out by Oberli *et al.* (2014), and as noticed during the present work, these imperfections act as nucleation points for ice accretion.

Results shown in the next section were obtained for mean flow velocity of 11.7 m/s and mean temperature of 20 ^{o}C for liquid water impacting flow and -6 ^{o}C for supercooled droplets impacting flow. In order to avoid water from freezing inside the nozzles, the compressed air inlet was kept open during the wind tunnel runs.

3. RESULTS

Five different tests were performed in order to characterize the water-repellant properties of the hydrophobic coating. The static contact angle was first measured by imaging a sessile drop sitting on the hydrophilic and on the hydrophobic surface. Next, using a syringe positioned at two different heights, an investigation at the dynamics of the

droplet impingement onto the control and coated surfaces was performed. The high speed camera images allowed to track the drop deformation, break up and re-bounce, depending on the impact velocity.

In addition, two experimental measurements were conducted at the Climatic Wind Tunnel. At first, flow temperature was kept above freezing conditions in order to observe the water repellant behavior of the surfaces. Next, negative temperatures were reached to observe the ice accretion phenomena.

3.1 Contact angle

The wettability of a solid surface can be characterized by the shape of a drop resting over it. Specifically, the wettability is characterized by the contact angle, i.e. the angle that is formed between the liquid solid and the liquid-vapor interfaces. A hydrophilic surface has high wettability, what means that the drop spreads over the surface it is sitting on. Low wettability implies hydrophobicity, when the drop tends to retain its spherical shape and can easily be shed from the surface by a slight vibration or tilt. According to Young's equation, Eq. (1), the contact angle θ can be derived by a balance in the surface tensions as:

$$Cos\theta = \frac{\gamma_{SV}-\gamma_{SL}}{\gamma_{LV}}, \tag{1}$$

where γ_{SV} is the surface tension between the solid and vapor. Further subscripts indicate the corresponding interfaces. According to Queré (2005), the contact angle for a flat surface cannot exceed 120°. When higher angles are observed it is implied that the surface is rough. The roughness valleys are filled with air so that the liquid has only partial contact with the top of the roughness elements. Surfaces can be classified as hydrophilic when $\theta < 90^o$, hydrophobic for the range $90^o < \theta < 150^o$, and superhydrophobic when $\theta > 150^o$.

It should be noted that when the roughness/heterogeneity of the surface is small compared to the size of liquid-vapor interface, the contact angle and its characterization is independent from droplet size according to Bhushan & Jung (2011).

Another parameter for wettability characterization is the contact angle hysteresis, Δθ, which is quantified as the difference between advancing and receding contact angles. According to Pierce *et al.* (2008), the measurement of contact angle is important for predicting drop shedding since the contact angle hysteresis is a measure of drop mobility and the equilibrium/advancing contact angle is a measure of repellency.

Using a small syringe, a single drop was placed to rest on a static surface (Figure 3). Then, the Shadow Sizer System described previously was used to capture high resolution images. Geometrical analysis of the droplets was performed using a CAD software in order to calculate the contact angles, as illustrated in Figure 4 - (a, b and c) for the case of hydrophilic surfaces and (d, e and f) for hydrophobic surfaces. The droplet is approximated to an ellipse – and to the particular case "circle" whenever possible. The substrate surface where the droplets rests was modelled as a straight line.

Figure 3: Sessile droplets sitting on a hydrophilic (right) and hydrophobic (middle) surfaces. On the left is a sketch indicating the definition of the contact angle.

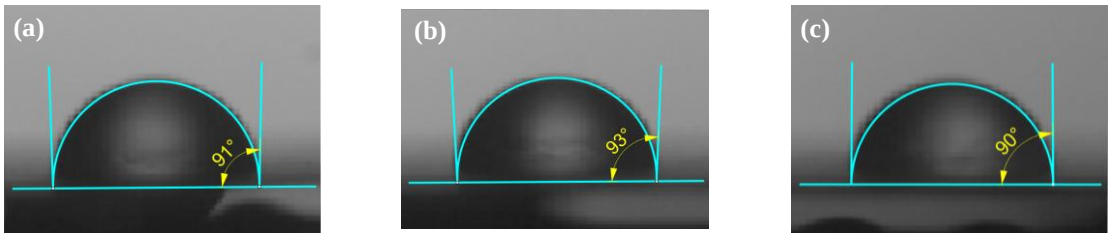

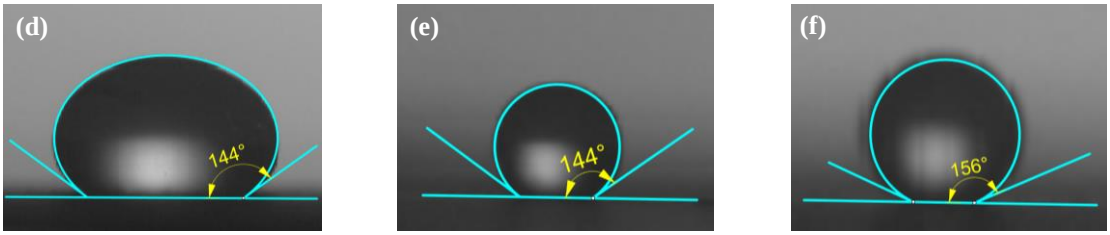

Figure 4: Contact angles measured for the hydrophilic (a, b and c) and hydrophobic (d, e and f) surfaces.

For the reference aluminum surface, the observed median contact angle was 91º, while for the coated surface a value of 144º was obtained, characterizing it as hydrophobic as expected.

3.2 Impact of a free falling drop on a surface

According to Pierce *et al.* (2008) and Antonini *et al.* (2008), two different mechanisms that promote icing mitigation can be identified: (i) partial or complete rebound of drop upon impact, with drop entrainment in a prevailing airflow; (ii) shedding of sessile drop, which is possible when liquid–surfaces adhesion forces are overcome by external forces (aerodynamic forces or gravity).

Figure 5 shows an illustration of eight images taken of a water droplet impinging on the smooth aluminum surface. The acquisition time is shown to each photo. The droplet starts to fall after 1.5808 s of acquisition. For the distance investigated (H = 18 mm), the impact is small and no droplet breakup is observed. For the same distance used in Figure 5, droplet bounces back after impinging on the hydrophobic surface, but again no break up phenomena is observed, as illustrated in Figure *6*. The acquisition time is shown in each photo. The droplet started to fall after 1.5808 s and 1.4733 s of acquisition for the hydrophilic and hydrophobic test, respectively. In both cases the measured velocity immediately before impact is 0.5 m/s.

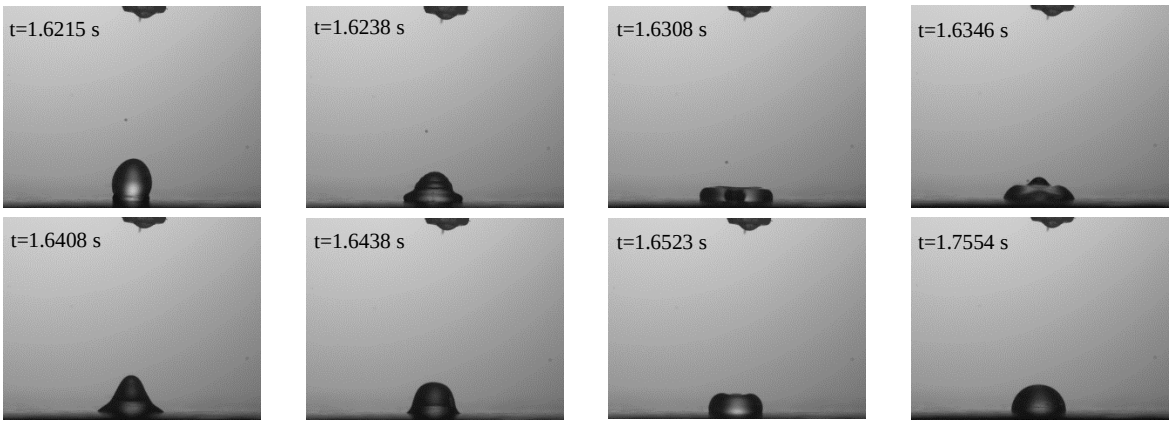

Figure 5: Droplet falling on a hydrophilic surface (H = 18 mm).

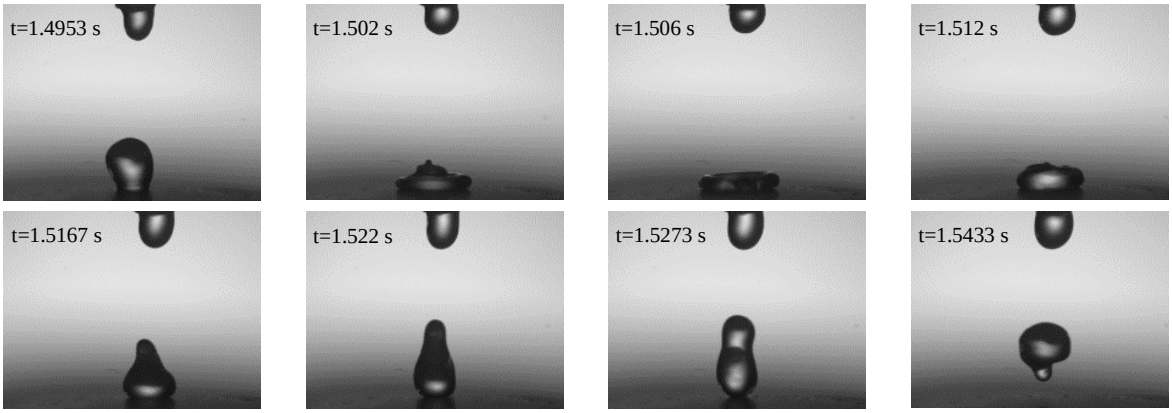

Figure 6: Droplet falling on a hydrophobic surface (H = 18 mm).

When the syringe was located at a distance of 240 mm from the surface (Figure *7*), the measured impact velocity was 3.7 m/s and now the impact causes the droplet to break up in numerous smaller particles. These smaller particles would have two different effects on ice accretion: under airflow conditions, they would be easily carried away from the surface, diminishing the chances of occurring ice accretion, but, on the other hand, since the small droplets have relatively larger areas, they also could freeze more quickly. This break up does not occur in the hydrophilic surface even for the 240 mm distance. In fact, the deformation is very similar to that observed in Figure 5, but with a larger spread. The acquisition time is shown in each photo. The first photo that captured the droplet falling was taken after 1.0177 s of acquisition.

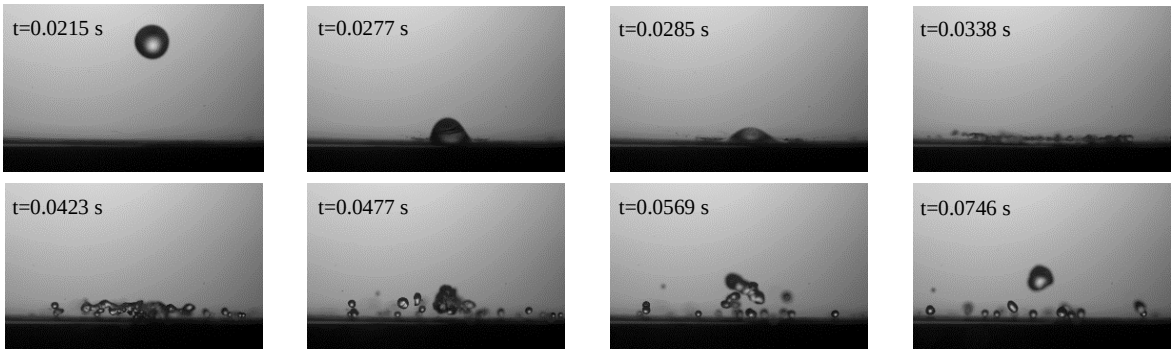

Figure 7: Droplet falling on a hydrophobic surface. (H = 240 mm).

3.3 Airflow over airfoil NACA0021

The Shadow Sizing technique was used to meaure the water droplets diameter distribution. The nozzles were working under room temperature (20°C) and air velocity was set to 11.7 m/s. The air pressure was kept at 3.2 bar while the water pressure was 2.2 bar. A total of 117 photos were taken, where 3,334 droplets could be identified. The median diameter was 0.194 mm with standard deviation of 0.042 mm, which falls under the category of large droplets, according to Wendisch *et al.* (2002). The results obtained are shown in Figure 8.

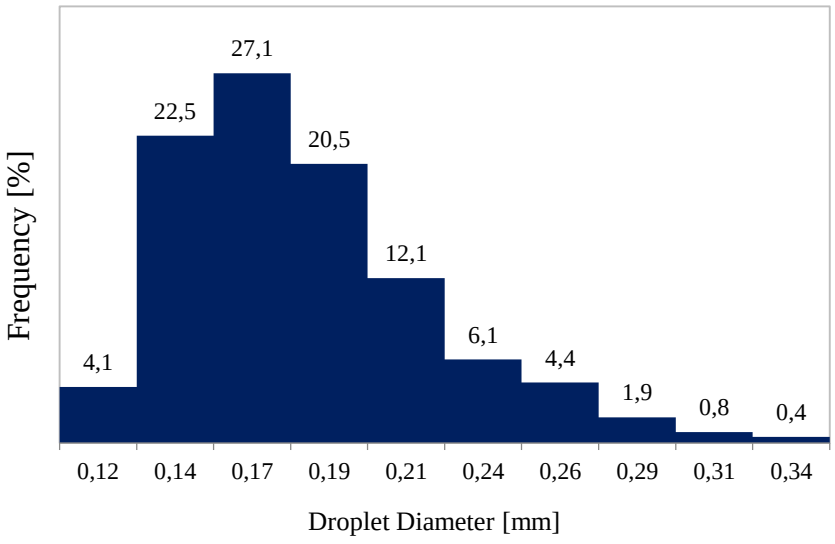

Figure 8: Droplet diameter histogram.

Figure 9 shows the droplets present in the flow impinging on the hydrophilic and hydrophobic profiles. The flow was set in the following conditions:

- Air pressure of the spray bar system: ~3.2 bar
- Water pressure of the spray bar system: ~2.2 bar
- Airflow mean velocity: 11.7 m/s
- Water droplet mean velocity: ~11.9 m/s
- Mean flow temperature: ~ 20 ºC

- Frequency of image acquisition: 1496 Hz
- Total acquisition time: 3.0 s
- Ambient temperature: ~18ºC

The water droplet mean velocity was also measured with the aid of the Shadow Sizer System. Indeed, the spray bar system operational condition is adjusted so that the water droplets reach the test section at approximately the same velocity of the mean airflow, which was monitored by a Pitot tube. The small difference of 2% between the mean airflow and droplet velocities lies within the uncertainty of the measurements.

Figure 9 shows the behavior of water droplets flowing around the hydrophilic airfoil (left column), in comparison to the hydrophobic model (center and right column). The images on the left column show that the water droplets that impinge on the airfoil are efficiently collect by the hydrophilic surface. The droplets eventually give origin to a film of water with instability waves that move over the airfoil surface and favors freezing. This wing reshaping by the ice accreted on the surface can lead to decrease lift and may lead to critical premature stalling.

Unlike the reference airfoil, for the hydrophobic profile (Figure 9 – center and right columns) no major surface wetting was observed. Water droplets attached to the airfoil surface exhibit a segregated configuration, with diameters similar to droplets within the external flow.

Shear forces exerted by the main flow can remove the attached droplets from the airfoil, mainly by two methods. The first consists of droplets being ejected by an experienced centrifugal acceleration for a non-inertial reference frame. When the outward centrifugal force is greater than the adhesion force between water and substrate, the droplet is detached and follows a path tangent to the profile surface (Figure 9 – center column). The second method comprises of droplets being removed from the surface upon colliding with other droplets. Some small regions of the airfoil lack hydrophobic paint due to wear through successive test trials or imperfections in the original paint, allowing droplets to stick on the substrate. Observations showed that those adhered droplets are removed by momentum exchange with other droplets dispersed in the external flow as can be seen on Figure 9 – right column.

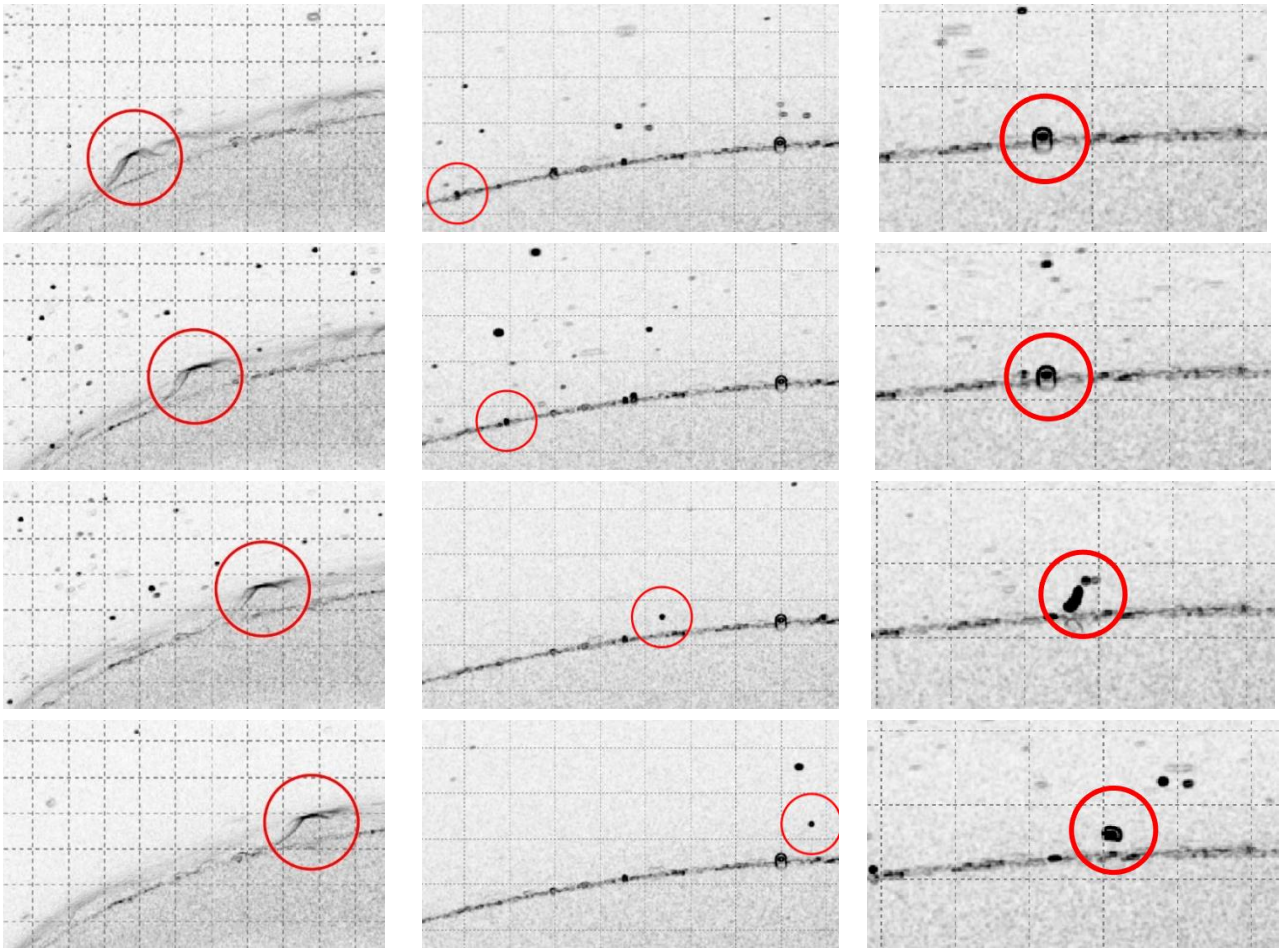

Figure 9: Clustering of droplets moving across hydrophilic (left column), time-step between images is 0.032s. Droplet being eject from hydrophobic surface (center and right columns), time-step between images is 0.010s. Flow from left to right.

Figure 10 and Figure 11 show, respectively, the profiles of the ice accreted on the hydrophobic and hydrophilic wings along a test run of 205.8 seconds (4116 frames acquired at 20 Hz). For this test, the temperature was

approximately -6.3 ºC. At the end of each experiment, the model was weighted in order to have a global estimate of the ice accumulated in each model. Results show that the hydrophilic model has accumulated 75.1 g of ice, against 28.5 g weighted on the hydrophobic surface. The difference in accumulated ice is about 2.6 times lower for the hydrophobic surface and the time delay in the start of ice accretion was 23 seconds, while for the aluminum airfoil the ice accretion initiated immediately. Qualitatively, the frame captured at 174.399 s, shows that significantly more ice has accreted on top of the airfoil.

Although the ice strength adhesion was not rigorously quantified in the course of these experiments, we could notice that the ice accreted on the hydrophobic surface could be easily removed (manually) after the run, what did not happen for the hydrophilic surface. However, the necessary shear force to remove ice regions on the surface is not achieved by the external airflow, as soon as liquid water freezes when attached to the cold surface. So while surface hydrophobicity has demonstrated efficacy as explained in detail, its icephobicity was not observed thoroughly. In that case, no discussion about the surface icephobic nature is supported by careful investigation.

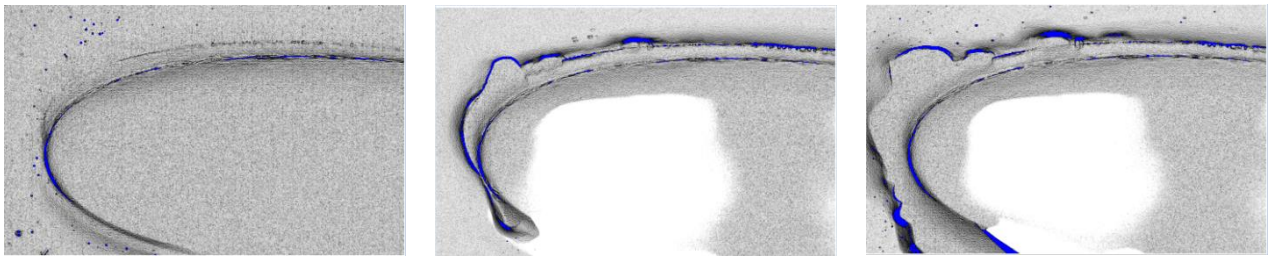

Figure 10: Shadow sizer images showing the profile of accreted ice on the hydrophobic wing: (a) 10.85 s; (b) 71.349 s and (c) 174.399 s.

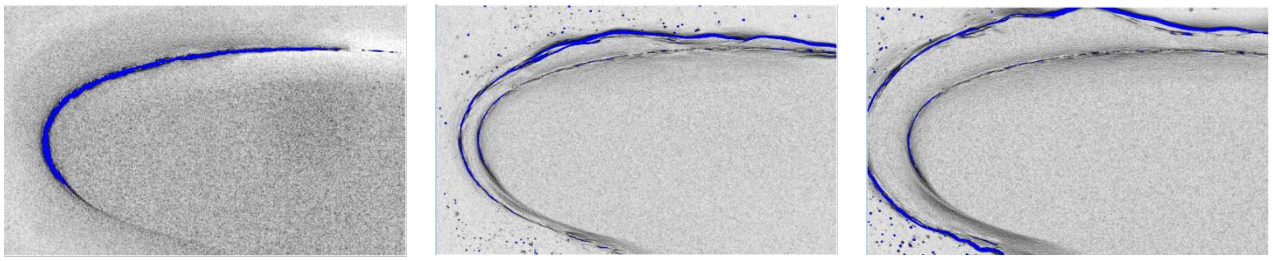

Figure 11: Shadow sizer images showing the profile of accreted ice on the hydrophilic wing: (a) 10.85 s; (b) 71.349 s and (c) 174.399s.

Figure 12 show the ice shape formed on the lower surface of the model wings. Over the hydrophilic aluminum airfoil (left), ice sticks to the whole surface, following the path of the liquid droplets shed by the main flow. On the right picture of Figure 12, it can be seen that ice is not accreted on the hydrophobic surface, although the growth of glaze ice gave origin to ice fingers caused by the shed liquid droplets (right).

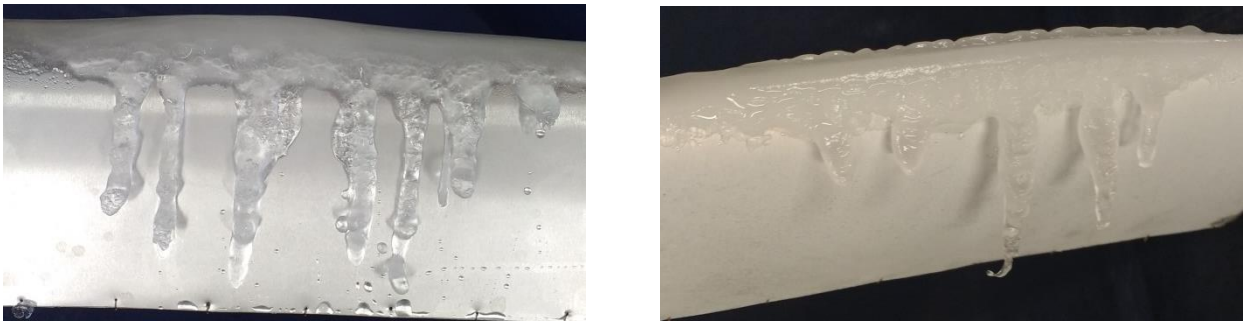

Figure 12: Ice accretion on the bottom surface of the aluminum wing (left) and on the hydrophobic surface (right).

A simple observation of the coating durability showed that, in between tests, the coated layer was gradually removed from the aluminum surface. Consequently, its hydrophobicity characteristics decreased over time, causing loss of ice prevention performance. According to Farhadi S. et. al. (2011), the durability of the material used for coating increases when composed by very hard or elastic rough structures.

5. FINAL REMARKS

This work has focused on the investigation of the effects that hydrophobic surfaces exert on the ice accretion phenomenon, considering the influence of the turbulent flow that drives the droplet impact. Experiments have been performed on the Climatic Wind Tunnel (NIDF/UFRJ) with the aid of a spray bar system that can simulate atmospheric supercooled large droplets. A commercial hydrophobic paint was used to coat an aluminum sheet that was further used to construct the hydrophobic airfoil. Results for contact angle and ice accreted shape were presented. The analysis of the hydrophobic-coated airfoil has been done in comparison to the reference aluminum airfoil. Future works will investigate the boundary layer structure very near to the surface in order to relate skin friction and roughness parameter to the water-repellant performance of hydrophobic surfaces.

6. ACKNOWLEDGEMENTS

LVF is grateful to the Brazilian National Research Council (CNPq) for the award of a PhD scholarship. In the course of the research, JBRL benefited from a CNPq Research Fellowship (Grant No 308445/2013-9) and from further financial support through Grants CNPq 458249/2014-9, FAPERJ E-26/102.212/2013 and FAPERJ E-26/010.002857/2014.

7. REFERENCES

Alizadeh, A., Yamada, M., Li, R., Shang, W., Otta, S., Zhong, S., Ge, L., Dhinojwala, A., Conway, V., Vinciquerra, A., Stephens, B. and Blohm, M., 2012. "Dynamics of Ice Nucleation on Water Repellent Surfaces." Langmuir. ACS Publications.

Antonini, C., Innocenti, M., Horn, T., Marengo, M., and Amirfazli M., 2011. "Understanding the effect of superhydrophobic coatings on energy reduction in anti-icing systems." Cold Regions Science and Technology. Elsevier, 58-67.

Bharathidasan, T., Kumar, S. V., Bobji, M. S., Chakradhar, R. P. S. and Basu, B. J., 2014. "Effect of wettability and surface roughness on ice-adhesion strength of hydrophilic, hydrophobic and superhydrophobic surfaces." Applied Surface Science. Elsevier, 241-250.

Bhushan B., Jung Y. C., 2011. "Natural and biomimetic artificial surfaces for superhydrophobicity, self-cleaning, low adhesion, and drag reduction." Progress in Materials Science 1-108.

Farhadi S., Farzaneh M., Kulinich S.A. 2011. "Anti-icing performance of superhydrophobic surfaces." Applied Surface Science 6264–6269.

Fortin, G., Adomou, M. and Perron, J., 2011. "Experimental Study of Hybrid Anti-Icing Systems Combining Thermoelectric and Hydrophobic Coatings". SAE International.

Lynch, F. T. and Khodadoust, A., 2001. "Effects of ice accretions on aircraft aerodynamics." Progress in Aerospace Sciences. Huntington Beach: Elsevier, 669-767.

Miller, D. R. and Harold Jr. E. A., 1996. "A study of large droplet ice accretions in the NASA Glenn IRT at near-freezing conditions." AIAA. Cleveland, Ohio.

Oberli, L., Caruso, D., Hall, C., Fabretto, M., Murphy, P. J. and Evans, D., 2013. "Condensation and freezing of droplets on superhydrophobic surfaces." Advances in Colloid and Interface Science. Elsevier, 47-57.

Pierce, E., Carmona, F. J. and Amirfazli, A., 2008. "Understanding of sliding and contact angle results in tilted plate experiments." Colloids and Surfaces A: Physicochemical and Engineering Aspects, 73–82.

Wendisch, M., Garrett, T. J. and Strapp, J. W., 2002: Wind tunnel tests of the airborne PVM-100A response to large droplets. J. Atmos. Oceanic Technol., 1577–1584.

8. RESPONSIBILITY NOTICE

The following text, properly adapted to the number of authors, must be included in the last section of the paper: The author(s) is (are) the only responsible for the printed material included in this paper.